Broadband dispersion compensation using inner cladding modes in photonic crystal fibers

Felipe Beltrán-Mejía,[1,2] Cristiano M. B. Cordeiro,[2] Pedro Andrés[1] and Enrique Silvestre[1,*]

[1]*Departamento de Óptica, Universidad de Valencia, 46100 Burjassot, Valencia, Spain*
[2]*Instituto de Física "Gleb Wataghin", Universidade Estadual de Campinas - UNICAMP, Campinas, SP, Brazil*

[*] *enrique.silvestre@uv.es*

Abstract: A photonic crystal fiber is optimized for chromatic dispersion compensation by using inner cladding modes. To this end, a photonic-oriented version of the downhill-simplex algorithm is employed. The numerical results show a dispersion profile that accurately compensates the targeted dispersion curve, as well as its dispersion slope. The presented fiber has a simple structure, while radiation losses can be reduced simply by adding a few more air-hole rings. Fabrication tolerances are also considered showing how fabrication inaccuracies effects can be overridden by just adjusting the compensation length.

OCIS codes: (060.4005) Microstructured fibers; (060.5295) Photonic crystal fibers; (230.2035) Dispersion compensation devices.

References and links

1. J. C. Knight, T. A. Birks, P. S. J. Russell, and D. M. Atkin, "All-silica single-mode optical fiber with photonic crystal cladding," Opt. Lett. **21**(19), 1547–1549 (1996).
2. A. Ferrando, E. Silvestre, J. J. Miret, P. Andrés, and M. V. Andrés, "Donor and acceptor guided modes in photonic crystal fibers," Opt. Lett. **25**(18), 1328–1330 (2000).
3. A. Ortigosa-Blanch, J. C. Knight, W. J. Wadsworth, J. Arriaga, B. J. Mangan, T. A. Birks, and P. S. J. Russell, "Highly birefringent photonic crystal fibers," Opt. Lett. **25**(18), 1325–1327 (2000).
4. J. M. Dudley, G. Genty, and S. Coen, "Supercontinuum generation in photonic crystal fiber," Rev. Mod. Phys. **78**(4), 1135–1184 (2006).
5. E. Silvestre, T. Pinheiro-Ortega, P. Andrés, J. J. Miret, and A. Coves, "Differential toolbox to shape dispersion behavior in photonic crystal fibers," Opt. Lett. **31**(9), 1190–1192 (2006).
6. A. Ferrando, E. Silvestre, J. J. Miret, and P. Andrés, "Nearly zero ultraflattened dispersion in photonic crystal fibers," Opt. Lett. **25**(11), 790–792 (2000).
7. A. Ferrando, E. Silvestre, P. Andrés, J. Miret, and M. Andrés, "Designing the properties of dispersion-flattened photonic crystal fibers," Opt. Express **9**(13), 687–697 (2001).
8. W. Reeves, J. Knight, P. Russell, and P. Roberts, "Demonstration of ultra-flattened dispersion in photonic crystal fibers," Opt. Express **10**(14), 609–613 (2002).
9. B. Eggleton, P. Westbrook, C. White, C. Kerbage, R. Windeler, and G. Burdge, "Cladding-mode-resonances in air-silica microstructure optical fibers," J. Lightwave Technol. **18**(8), 1084–1100 (2000).
10. W. H. Press, S. A. Teukolsky, W. T. Vetterling, and B. P. Flannery, *Numerical recipes in C (2nd ed.): the art of scientific computing* (Cambridge University Press, New York, NY, USA, 1992), chap. 10, pp. 408–412.
11. F. Poletti, V. Finazzi, T. M. Monro, N. G. R. Broderick, V. Tse, and D. J. Richardson, "Inverse design and fabrication tolerances of ultra-flattened dispersion holey fibers," Opt. Express **13**(10), 3728–3736 (2005).
12. J. C. Lagarias, J. A. Reeds, M. H. Wright, and P. E. Wright, "Convergence properties of the nelder–mead simplex method in low dimensions," SIAM J. Optimiz. **9**(1), 112–147 (1998).

13. S. Cui, D. Liu, S. Yu, B. Huang, C. Ke, M. Zhang, and C. Liu, "Downhill simplex algorithm based approach to holey fiber design for tunable fiber parametric wavelength converters," Opt. Express **18**(10), 9831–9839 (2010).
14. Corning© LEAF© optical fiber. Product Information (Corning Inc., N.Y. 2009).
15. K. Thyagarajan, R. Varshney, P. Palai, A. Ghatak, and I. Goyal, "A novel design of a dispersion compensating fiber," IEEE Photonic. Tech. L. **8**(11), 1510–1512 (1996).
16. T. Fujisawa, K. Saitoh, K. Wada, and M. Koshiba, "Chromatic dispersion profile optimization of dual-concentric-core photonic crystal fibers for broadband dispersion compensation," Opt. Express **14**(2), 893–900 (2006).
17. S. D. Gedney, "An anisotropic perfectly matched layer-absorbing medium for the truncation of FDTD lattices," IEEE T. Antenn. Propag. **44**(12), 1630–1639 (1996).
18. A. Oskooi and S. G. Johnson, "Distinguishing correct from incorrect PML proposals and a corrected unsplit PML for anisotropic, dispersive media," J. Comput. Phys. **230**(7), 2369–2377 (2011).

1. Introduction

Photonic crystal fibers (PCF) are optical fibers with a transversal array of air-holes that extends along all the fiber's length [1]. PCFs optical guiding is due to the multiple interference caused by the periodical array of air-holes and also by the high index contrast between silica and air [2]. The rich geometry of the fiber's microstructure and its complex wave-guiding mechanism makes PCFs the suitable choice for a great deal of applications such as dispersion compensators, interferometers, super-continuum generators and polarization maintainers between others [3–5]. Up to now, the dispersive behavior on PCFs have been studied thoroughly for the core modes [6–8]. In comparison, little has been deepened in higher order modes propagating through the cladding of a PCF [9], despite of the geometrical richness and the dispersion control provided by their cladding structures.

In this work we present, as an example of realistic applications using inner cladding modes, a dispersion compensating fiber with a very low residual dispersion. To fulfill this goal, a photonic-oriented version of the downhill-simplex algorithm [10] — utilizing a proper scaling rule for dispersion — has been implemented and is presented here along with the results of the optimization process and the fabrication tolerances for the proposed fiber (Fig. 1). The adapted procedure considerably speeds the pace towards convergence, giving a more optical criteria to shorten the way through the optimization process. Comparisons will show the benefits of the introduced modifications, followed by the results obtained for the compensating PCF using inner cladding modes. In addition, a complete analysis of the fabrication tolerances and the radiation losses is presented for the proposed fiber. Finally, the benefits and disadvantages of this approach will be discussed along with the conclusions of this proposal.

2. Photonic-oriented optimization method

Since there is a considerable number of parameters involved in the optimization of the performance of a microstructured fiber (e.g., different air-hole diameters, lattice pitch, and others), it is convenient to get hold of the right tool previous to deal with the optimization process of the fiber structure. Many methods are available for tackling this task, and some of them has been used for optimizing guiding microstructures, as it is the case of stochastic or genetic algorithms [11] or those based on the knowledge of first derivatives [5]. The downhill-simplex method has been successfully applied to optimize optical applications such as fiber lasers or nonlinear wavelength converters, as well as in chemistry, mechanical engineering, biomedical imaging, geophysics among others fields where a multidimensional unconstrained minimization is required [12, 13]. Its geometric nature makes it suitable for customizations as well as combinations with other optimization methods. Here we adapted this method for a concrete objective, a compensating fiber, obtaining acceptable results with a low investment of computation time. Although, it is worth to point out that this enhancement does not rely on any detail of the algorithm, therefore is independent of the optimization method.

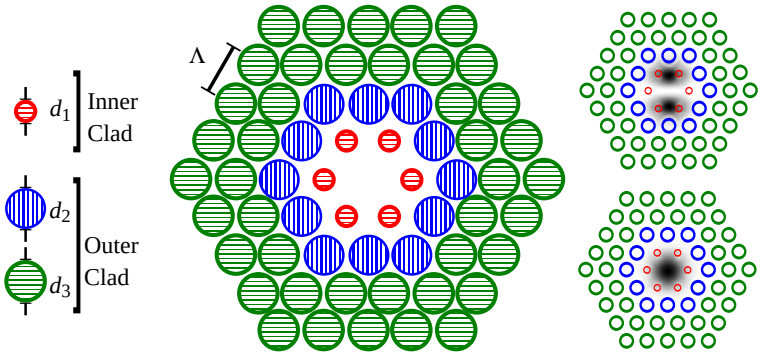

Fig. 1. (Color online) Left, initial fiber structure used during the optimization process. Right, one of the LP_{11} modes used here for dispersion compensation and a fundamental mode, LP_{01}, for illustration purposes.

In our case, in order to compensate the chromatic dispersion of a certain distance of a given standard single mode fiber (SMF) with the unity distance of a compensating fiber, we define a merit function

$$\chi^2[P] = \sum_{\lambda} \{D[P](\lambda) + X\, D_{\mathrm{SMF}}(\lambda)\}^2, \tag{1}$$

where D_{SMF} and $D[P]$ are the dispersion profiles of the single mode fiber and the compensating fiber respectively; both must have opposite signs in order to minimize χ^2. The vector $P = (p_1, \ldots, p_N)$ represents a given configuration defined by N design parameters, p_i, and X is the compensation factor, that is, the ratio between the lengths of the SMF and the compensating fiber. In Eq. (1), the expression between curly brackets is proportional to the residual dispersion of the whole system and the sum is performed over a finite number of wavelengths in the design interval (the C band, $1530\,\mathrm{nm} \leq \lambda \leq 1565\,\mathrm{nm}$).

In the search for a minimum of the merit function, the downhill-method uses $N+1$ points as vertices to construct a geometrical object, the *simplex*, that evolves in the quest for the lowest point in the N-dimensional parameter space. The search for configurations with lower values of χ^2 includes several geometrical strategies around the lowest point to go "downhill" through the merit function. Every step in the algorithm tries to replace the worst vertices — with higher values of χ^2 — of the simplex with other points presenting lower values of the merit function. In this way the simplex always brings together the set of the best $N+1$ fibers of all those who have been examined through the optimization process. That makes the downhill-simplex method an effective and easy to use optimization technique, appropriate when the derivate of the merit function is not available or is expensive to obtain.

However, it must be taken into account that any attempt of substituting a point of the simplex implies the evaluation of the merit function at the candidate point to be included in. And, as the fiber structure grows in complexity, the space of parameters and the optimization procedure raise in dimensions and in computation time respectively. To lessen this disadvantage the downhill-simplex algorithm can be customized with an extra step that fastens the convergence. This new kind of step is based on the magnification, M, of the structure, a geometrical transformation that has a special relevance since strongly affects optical systems. If the total dispersion of a given configuration, $D[P]$, is known, an accurate nonlocal approximation for the structure magnified by a factor M, is given by

$$D[MP](\lambda) \approx \frac{1}{M}\left\{D[P]\left(\frac{\lambda}{M}\right) - D_m\left(\frac{\lambda}{M}\right)\right\} + D_m(\lambda), \tag{2}$$

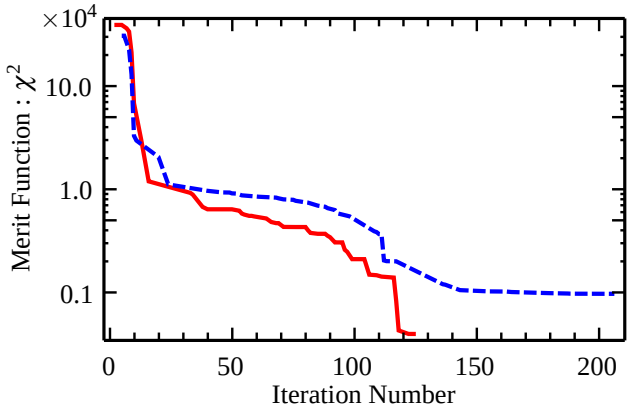

Fig. 2. (Color online) Fitness function vs. number of iterations for the in-house (solid red) and the conventional (dashed blue) simplex algorithm.

where D_m is the material dispersion [5]. This expression significantly improves the previous scaling formula for the group velocity dispersion reported in Ref. [6].

Equation (2) establishes a simple link between different points in the configuration space that deserves to be exploited. This link can be noticed more clearly if the parameter space is broken into different hyperplanes where $M = \Lambda/\Lambda_0$ is constant, where Λ is a typical distance in the structure, e.g., the pitch. Then the optimization algorithm will seek only into one hyperplane at the time, while Eq. (2) efficiently determines which hyperplane – or equivalently M – is more appropriate to minimize χ^2. In this way, if we replace $D[P]$ with $D[MP]$ in Eq. (1), the original optimization algorithm can be applied to simplices defined in those hyperplanes made up of only N vertices.

On the other hand, minimizing χ^2 with respect to M is a straightforward procedure using Eq. (2). At the end of each iteration, the value of M which minimize χ^2 at one of the vertices is determined, and then the whole simplex at the current hyperplane can be transferred to the new hyperplane at a negligible computational effort. As an example of the enhancement obtained using this procedure, Fig. 2 shows how it overcomes the conventional algorithm [10].

3. Inner cladding modes for dispersion compensation

The procedure sketched in the previous section has been applied to the optimization of a compensating PCF. As it is shown in Fig. 1, the PCF has four air-hole rings with three different air-hole diameters. The most inner ring, with air-holes of diameter d_1 (red circles), constitutes the inner clad. The other air-hole rings, of diameter d_2 and d_3 (blue and green circles) constitute the outer clad, being all the air-holes arranged in a triangular lattice of pitch Λ. The modes used for dispersion compensation will be LP_{11} modes that propagates along the inner clad of the PCF.

The values for the initial parameter vector were $P_0 = \{\Lambda_0, d_1, d_2, d_3\} = \{1.05\,\mu m, 0.46\,\mu m, 2d_1, 2d_1\}$. Around these values four other vectors representing other triangular PCFs were randomly chosen as vertices of the simplex described in the initial hyperplane, $\Lambda = \Lambda_0$, or equivalently $M = 1$. At the end of the optimization process, the obtained fiber configuration should compensate the dispersion of a Corning LEAF fiber [14] multiplied by the compensation factor X set to 100 [see Eq. (1)]. The initial design was inspired on Dual Concentric Core Fibers (DCCF) [15, 16] which have shown to be a successful design for achieving highly negative dispersion curves despite it has only been used, up to our

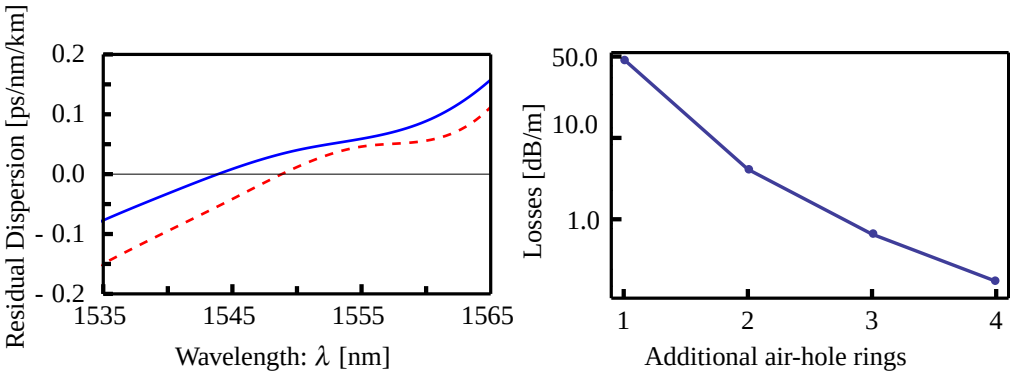

Fig. 3. (Color online) (a) Residual dispersion for the optimized fiber with four (dashed red) and seven (solid blue) air-hole rings. (b) Radiation losses as a function of the additional rings included at the periphery of the cladding.

knowledge, for central core modes applications. It was set in this way to constrain the amount of modes that can be excited into the internal clad while the final result of the optimization process was not conditioned to maintain this configuration. Although the proposed structure is not original, it is simpler than previous ones used for this purpose.

For the adapted downhill-simplex method, a satisfactory fitness value was obtained after 122 evaluations while the conventional algorithm was stagnated in a superior local minimum (see Fig. 2). Though this amount of evaluations seems considerable, it is not if it is compared with stochastic algorithms [11]. The resulting PCF with $P = \{0.851, 0.322, 0.794, 0.638\}\,\mu m$ has a RMS value of the residual dispersion of $0.098\,\mathrm{ps/nm/km}$. The residual dispersion represented by the red dashed curve in Fig. 3(a) shows the low dispersion remaining in the system after compensating 100 km of the single mode fiber with 1 km of the proposed fiber. This could be further improved, as it is shown by the blue solid curve, with a final refinement made after knowing the results of the analyzes done for the radiation losses and the fabrication tolerance as presented below. Moreover, the slope of both curves are nearly zero at the 1555 nm region, therefore it also compensates higher order dispersions such as the dispersion-slope. This fact does not seems to be hampered by small deviations on the design parameters as will be shown in the next section.

If radiation loss is an issue, additional external air-hole rings could be included without appreciably affecting the fiber's dispersion profile. Also, with the aid of Eq. (2), M could be readjusted to fit the targeted dispersion. Figure 3(b) illustrates how by adding extra air-hole rings, with diameter d_2, radiation loss systematically decreases. Numerical results for the radiation losses where performed using the PML method [17], whose implementation was validated and tested by a recent procedure [18]. The blue solid curve in Fig. 3(a) shows how well the configuration could be re-optimized using Eq. (2); a rescaling of just $M = 1.014$ was needed after adding three outer rings with air-hole diameter d_2.

Finally, the recording of a Long Period Grating that excites the fundamental mode coming from the SMF fiber to the cladding mode LP_{11} of the compensating fiber, should not be demanding since the effective indexes of the lower order modes are well separated. As a matter of fact, the difference between the effective index of the LP_{01} and the LP_{11} modes (see Fig. 1) was $\Delta n_{\mathrm{eff}} = 0.122$, while for the LP_{11} and the LP_{02} modes was $\Delta n_{\mathrm{eff}} = 0.051$.

4. Fabrication tolerances

In the same way as the cladding structure conspicuously casts the dispersive properties of the fibers, it can also be a disadvantage when considering the fabrication tolerances. After analyzing

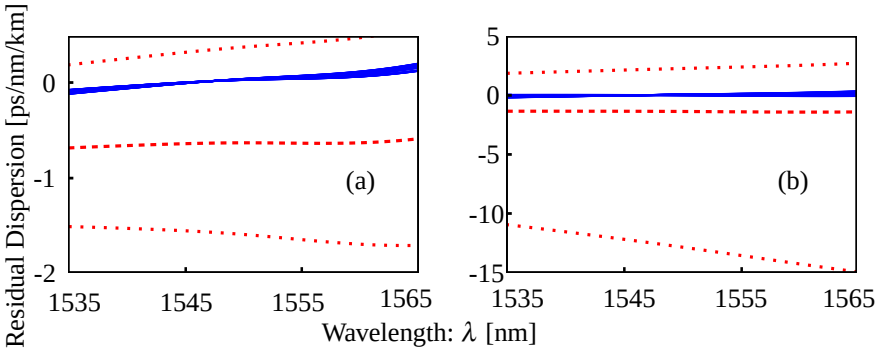

Fig. 4. (Color online) Residual chromatic dispersion for the optimized fiber (dashed red curve) delimited by the maximum deviations calculated for tolerances of (a) $\pm 1\%$ and (b) $\pm 5\%$ (dotted red curves). The residual dispersion was severely reduced by adjusting the free parameter X in Eq. (1) (solid blue bundled curves); differences between all the considered configurations can not be appreciated within these scales.

all possible cases of fabrication inaccuracies with a 5% maximum deviation, we noticed that the worst were those cases that formed an unrealistic combination between enlargement for some parameters and contraction for the others. The maximum tolerance narrows after discarding these spurious cases, realistically describing the plausible fabrication inaccuracies. On Fig. 4, dotted red curves delimit the allowing fluctuations of up to 1% (a) and 5% (b) on M, d_1, d_2 and d_3. Notice that for 5% tolerances, simultaneous fluctuations in the parameters of the proposed configuration in M and d_i implies that the accumulated deviations can exceed a 10% of inaccuracies, hampering noticeably the dispersion compensation. Fortunately, as it is well known, the factor X that multiplies the targeted dispersion in (1) is also a free parameter, thus, it can be conveniently adjusted to minimize the impact of the fabrication tolerances. In that way the residual dispersion was severely reduced as it is shown by the tight bundled solid blue curves in Figures 4 (a) and (b). The change applied to X for the different configurations range from 90.4 to 100.2 and from 65.5 to 182.5 for 1% and 5% tolerances respectively.

5. Conclusion

Albeit exciting cladding modes implies an additional complexity for fiber dispersion compensators, we have demonstrated that they can be used to precisely tailor the dispersion profiles needed to minimize the residual dispersion along with the third order dispersion. We have obtained low residual dispersions in the whole C band, even by using a high compensation factor and considering up to a 10% tolerance in the fabrication parameters. Moreover, the proposed structure has a simple geometry compared with others DCCFs that have been proposed in the literature [15, 16]. Also, since the compensating-cladding modes are isolated from the fundamental and other higher order modes, grating recordings may not be too demanding. To achieve these results, a well known optimization method has been adapted using an approximate analytical expression for magnification. The benefits of the optimized algorithm are a higher convergence speed while stagnation problems are reduced.

6. Acknowledgments

This work has been financially supported by the Brazilian agencies FAPESP and CAPES, and the Spanish Ministerio de Educación y Ciencia and Generalitat Valenciana (grants TEC2008-05490 and PROMETEO2009-077). F. Beltrán gratefully acknowledges financial support from FAPESP (grant 2011/01524-8).